Incorporation of transmissive scene element modeling in multispectral image simulation tools

R.V. Raqueño, S.D. Brown, and J.R. Schott

Digital Imaging and Remote Sensing Laboratory
Chester F. Carlson Center for Imaging Science
Rochester Institute of Technology
Rochester, New York

ABSTRACT

In order for advanced image simulation systems to properly model the image formation phenomenology of remotely sensed imagery, simulations need to account for the effects of transmissive objects in a scene. These transmissive effects are important in simulating imagery of littoral scenes, vegetation canopies, meteorological clouds, and gas plume discharges. This is especially true for imaging scenarios in the long wave infrared region where very complex target-background radiational and thermal interactions are critically affected by transmission. The Digital Imaging and Remote Sensing (DIRS) Laboratory's Synthetic Image Generation (DIRSIG) model has recently been improved to include the general simulation of transmissive scene elements. The model emphasizes quantitative prediction of the radiance reaching sensors with bandpass ranges between 0.28 and 20 μm. It includes spectral radiation propagation using MODTRAN, thermal modeling based on the environmental history, and extensive target-background interactions. An overview of DIRSIG's capabilities is presented along with the methodology and mechanism of simulating transmissive scene elements. Imagery illustrating the various scenarios and imaging phenomenologies are presented and discussed.

Keywords: Multispectral Image Simulation, Thermal Infrared Image Simulation, Cloud Simulation, Plume Modeling Simulation, Vegetation Canopy Simulation, Littoral Scene Simulation

1.0 Introduction and Background

This paper describes the techniques and improvements that have recently been incorporated into the multi-spectral image simulation tool-DIRSIG. It discusses the importance of transmissive scene elements and highlights the techniques that are currently implemented in the synthetic image generation process. Examples illustrating the various concepts are presented in each of the subsequent sections.

The advent of synthetic image generation (SIG) models has provided scientists and engineers in various disciplines powerful tools to analyze the numerous factors influencing the image formation chain. The quality and utility of image data as input to other analytical applications is governed by the ability to understand and account for these imaging factors (*e.g.* atmospheric attenuation, system MTF, SNR, *etc.*). SIG models offer a method to quantify these parameters for both forward and inverse modeling scenarios throughout the imaging process. In the forward modeling case, SIG provide a means to determine the detectability of a given physical phenomenon for a specific, well defined image acquisition scenario. Such a capability is invaluable in the design stage of sensors systems whereby engineers are given the facility to "build" a virtual imaging system from a given set of hypothetical specifications and test their performance under various operational conditions. This type of systems analysis can be accomplished prior to the assembly of an expensive physical prototype allowing changes and improvements to be made early in the design stage. SIG can also provide important mission planning and tasking support by predicting target detectability and image quality prior to the commitment of resources for a given mission. Conversely, SIG models allow verification of inverse models at the image analysis phase whereby observed targets requiring confirmation relating to material characteristics, surrounding atmospheric conditions, and/or imaging system performance can be determined. In this situation, SIG can predict for the analysts the resulting imagery based on interactive modifications of target and scene parameters.

Much of the focus of SIG models to date has been to visualize scenes containing man-made targets such as vehicles, buildings, and industrial complexes. These particular targets are characterized by well defined forms

0-8194-2216-9/96/$6.00

and well behaved material and optical properties. Demand for realism has required the incorporation of natural scene elements along with their radiometric influences on the entire scene. The state of the art of SIG has reached the level of realism where improvements to the reproduction fidelity of actual scenes requires the incorporation and modeling of the more subtle scene interactions produced by these natural scene elements. Of these interactions, transmission effects of both targets and backgrounds have subtle, but significant effects on the imagery. The next section will discuss the nature of these effects and the improvements that have been implemented to incorporate these phenomena.

2.0 DIRSIG

The specific SIG model of interest is DIRSIG (Digital Imaging and Remote Sensing Image Generation). It is a multipurpose simulation research tool developed to provide quantitative radiometric modeling of various multi-spectral imaging sensors. The scene is created and attributed using a CAD package which is then rendered by a ray-tracer submodel. Its spectral capability ranges from 0.3 to 20.0 microns with spectral resolution limits of 2 cm^{-1} as dictated by the current spectral limitations of MODTRAN3. It includes a thermal submodel (THERM) that predicts the diurnal temperature cycles for every pixel, based on environmental and meteorological inputs.[1] It also has the capability of simulating images from various sensor geometries including frame, push broom, and line scanner configurations.[2] Figure 1 represents an example of the model's current capabilities by showing a side by side comparison between a real thermal infrared line scanner imagery of the Hawkeye plant in the downtown area of Rochester, NY and a corresponding simulated scene generated by DIRSIG.[3]

Figure 1 - (Left) Bendix infrared line scanner imagery of Hawkeye Plant, Driving Park bridge, and Genesee River gorge in downtown Rochester, New York.
(Right) DIRSIG simulated imagery of corresponding region based on similar sensor parameters and atmospheric conditions.

DIRSIG's roots began as a simple analytical tool to model the target-background interaction physics explaining the resulting image phenomenology observed in the longwave infrared region. As it evolved to incorporate more complex interactions and sophisticated submodels, DIRSIG became mature enough to warrant validation studies in the longwave and midwave thermal infrared regions.[4] As a result of these validation studies, discrepancies were identified between the simulated and actual scenes due in part to the model's inadequate treatment of transmissive scene elements - in particular, meteorological clouds, which in the thermal infrared region, acted both as a source of radiation and as an attenuating medium. As a result,

scene elements such as background clouds significantly affect the resulting imagery even if these elements are not in the field of view of the sensor. Their proximity to the scene can significantly influence primary and sources such as solar irradiance and downwelled sky radiance.

In order to address this shortcoming, a generalized approach was conceived to provide the capability to rigorously account for the radiometric effects of the spectral transmission and emission properties of these special scene elements. The intent is not to model the microstructure physics of scene element transmission effects, but to provide a mechanism through which DIRSIG can accept a broad range of inputs from specialized models of material optical properties/processes and allow DIRSIG to propagate these small scale local effects to a macroscopic and synoptic level. The following section will detail the aspects of the governing radiometry equation and how it was modified to incorporate the transmissive scene elements.

3.0 Radiometry of DIRSIG Transmissive Scene Elements.

As a foundation to understanding the implementation of spectral transmission into DIRSIG, the baseline governing equation will be introduced. In order to understand the synthetic image generation process, it is first necessary to understand the physics and underlying principles that are involved in the capture of a real image. The first step is to visualize how the observed electromagnetic radiation ultimately reaches the sensor. The observed radiance at the front end of the sensor is comprised of eight different photon paths. The following diagrams show the different paths that electromagnetic radiation may travel before reaching the sensor. The first diagram shows the radiation originating from solar photons while the second diagram shows the radiation resulting from self-emission by the objects.

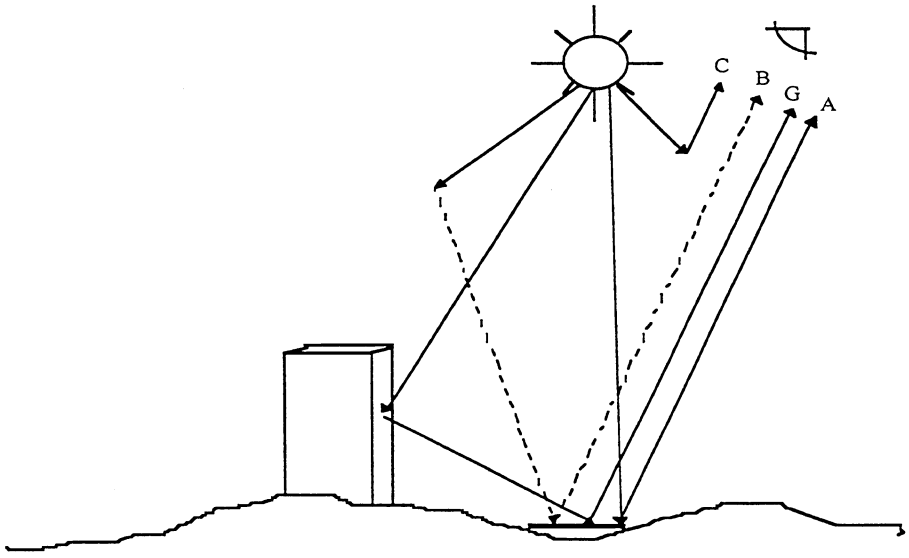

Figure 2 - Solar energy photon paths

Type A - Directly reflected solar photons attenuated by the atmosphere and clouds
Type G - Solar Photons reflected from the background onto the target
Type C - Solar photons scattered by the atmosphere
Type B - Solar photons scattered by the atmosphere onto the target

$$L_{solar} = A_{photons} + B_{photons} + G_{photons} + C_{photons}$$
$$= E' \cos\sigma' \frac{r}{\pi}\tau_1\tau_2 + F \cdot E_{ds\lambda}\frac{r}{\pi}\tau_2 + (1-F)\cdot L_{bs\lambda} r_d \tau_2 + L_{us\lambda} \quad (1)$$

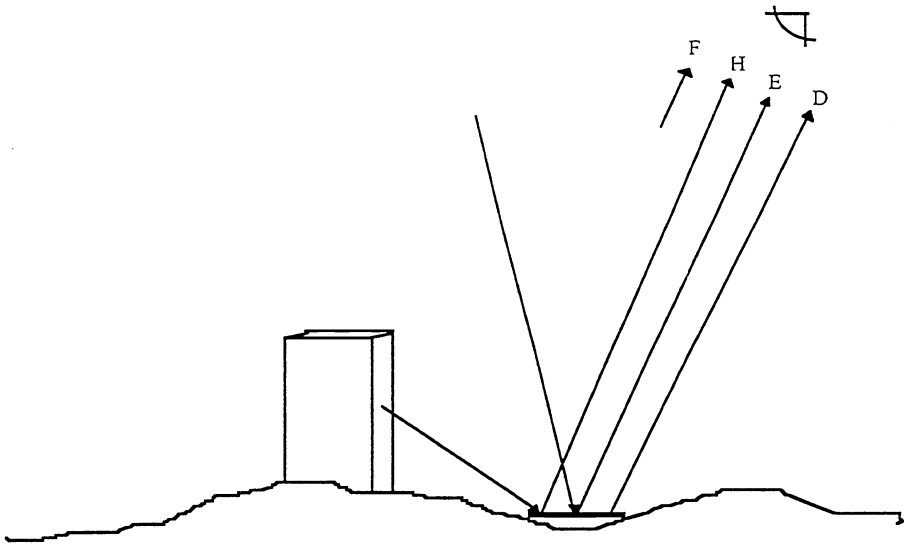

Figure 3 - Self-emitted energy photon paths

Type D - Self-emitted photons from the target attenuated by the atmosphere
Type E - Self-emitted photons from the sky reflected by the target to the sensor
Type F - Self-emitted photons from the atmosphere
Type H - Self-emitted photons from the background reflected by the target to the sensor

$$\begin{aligned} L_{\text{self-emission}} &= D_{\text{photons}} + E_{\text{photons}} + H_{\text{photons}} + F_{\text{photons}} \\ &= \varepsilon L_{T\lambda}\tau_2 + F\cdot\frac{r_d}{\pi}E_{d\varepsilon\lambda}\tau_2 + (1-F)r_d\cdot L_{b\varepsilon\lambda}\tau_2 + L_{u\varepsilon\lambda} \end{aligned} \tag{2}$$

After combining these two equations, $L_\lambda = L_{solar} + L_{self\text{-}emission}$, the total spectral radiance reaching the sensor can be described by the following equation.

$$\begin{aligned} L_\lambda = E_s' \cos\sigma' \frac{r(\lambda)}{\pi}\tau_1(\lambda)\tau_2(\lambda) + \varepsilon(\lambda)L_{T\lambda}\tau_2(\lambda) + F[E_{ds\lambda} + E_{d\varepsilon\lambda}]\frac{r_d(\lambda)}{\pi}\tau_2(\lambda) + \\ (1-F)[L_{bs\lambda} + L_{b\varepsilon\lambda}]r_d(\lambda)\tau_2(\lambda) + L_{us\lambda} + L_{u\varepsilon\lambda} \end{aligned} \tag{3}$$

E_s' - Exoatmospheric irradiance
$\cos\sigma'$ - the angle from the target normal to the sun
τ_1 - transmission of the atmosphere from the sun to the target
τ_2 - transmission of the atmosphere from the target to the sensor
$\varepsilon(\lambda)$ - target emissivity
$L_{T\lambda}$ - self-emitted radiance from target at temperature T
$E_{ds\lambda}$ - solar downwelled irradiance
$E_{d\varepsilon\lambda}$ - self-emitted downwelled irradiance from the sky
F - shape factor (amount of sky hemisphere that the target can see)
$1\text{-}F$ - the percentage of the atmosphere that is blocked by the background object
$r_d(\lambda)$ - target reflectance
$L_{bs\lambda}$ - background radiance from scattering
$L_{b\varepsilon\lambda}$ - background radiance from self emission
$L_{us\lambda}$ - upwelled radiance due to scattering of the atmosphere
$L_{u\varepsilon\lambda}$ - upwelled radiance due to the self emission of the atmosphere

This equation represents all the sources of radiation that are of significant importance in determining the radiance that reaches imaging systems sensitive to 0.3-14.5μm wavelengths. As noted, this equation is dependent upon the wavelength. Depending upon the spectral sensitivity of the imaging system, this equation may be simplified by neglecting certain terms since their effects are minimal at those wavelengths

The above equation represents the interactions found in scenes containing strictly opaque materials which limits the number of the photon paths and the branching at each interaction point. This is illustrated in Figure 4 where a sample diagram of source-target-sensor photon paths are represented as a ray-facet interaction tree diagram.

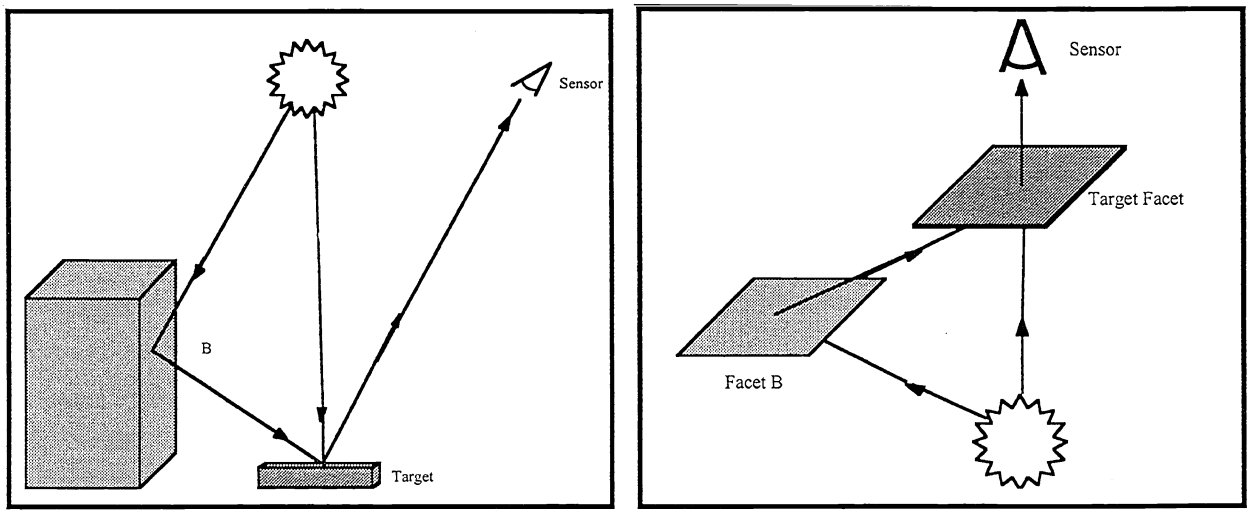

Figure 4 - Sample ray-facet interaction diagram and corresponding tree representation for opaque only case.

This tree diagram graphically represents the branches of photon paths at different stages of interaction with scene facets. It models and accounts for all scattered and emitted photons ultimately reaching the sensor. For the opaque case, the resulting tree diagram has a fixed maximum depth and breadth (i.e. a fixed maximum number of photon paths and facet interactions) and can be computed using Equation (3). The logic necessary for the computation can be represented by a handful of conditional cases. The introduction of transmissive scene elements, however, potentially increases the maximum depth and breadth of the ray-facet interactions as illustrated in Figure 5.

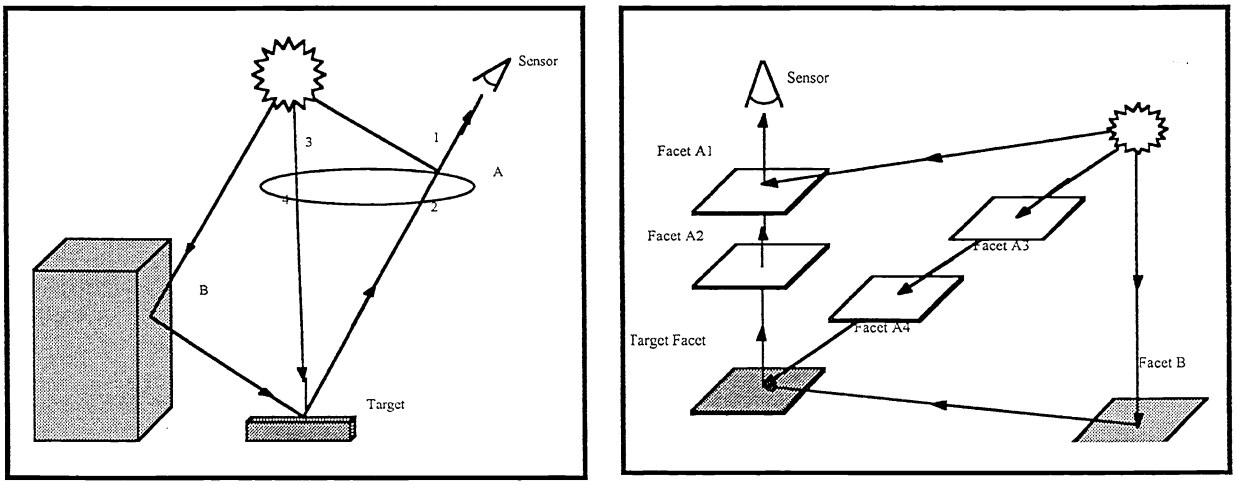

Figure 5 - Sample ray-facet interaction diagram and corresponding tree representation for transmissive and opaque case .

In this case, a scene element that represents a transmissive object is added to the previous scene of strictly opaque objects resulting in a significant increase in the ray-facet interaction tree. The addition of even a relatively few transmissive scene elements such as those shown in Figure 6 will result in ray-facet interaction configuration that can only be computed tractably by a recursive procedure where the contribution of each branch is computed in a bottom up approach toward the sensor. Conceptually, the contribution of each branch of the tree is computed by positioning the sensor at each branch and propagating the resulting interaction with the facet up the upper levels of the tree until it reaches the final sensor location.

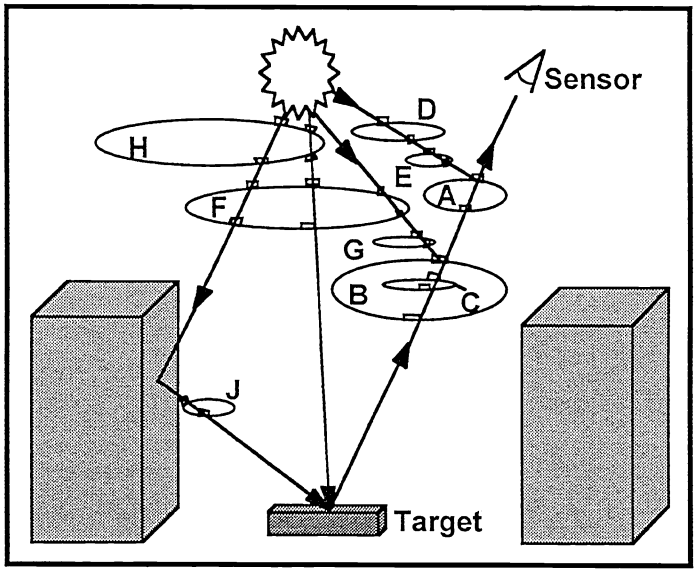

Figure 6 - More complex ray-facet interactions diagrams for multiple transmission objects and embedded transmission objects

The structure of transmissive scene elements implemented in DIRSIG are categorized into two type of facets - the Uniform Thickness Transmission Layer (UTTL) and the Nonuniform Thickness Transmission Layer (NTTL) illustrated in Figure 7.

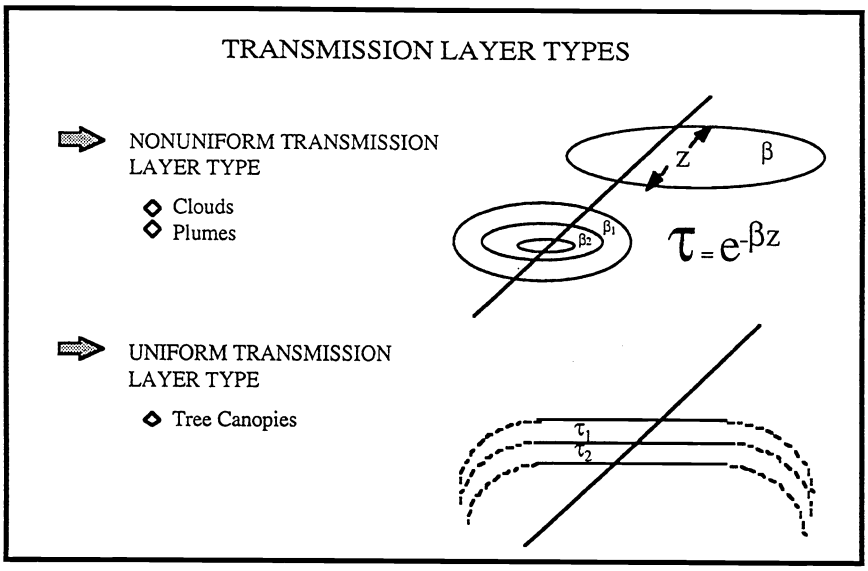

Figure 7 - Diagram of UTTL and NTTL cases and their corresponding applications

The UTTL facet was designed to model facet elements that effectively have a uniform thickness and homogeneous material properties for that facet element. This potentially decreases the complexity of assembling a particular scene by reducing the number of facets required to represent a transmissive element. Scenes containing leaves to form a forest canopy are modeled in DIRSIG using this type of transmissive element. The NTTL, represented by a set of facets defining a boundary surface enclosing a volume of homogeneous material properties, was designed to model more complex objects such as clouds and exhaust plumes (the form is similar to data structures used by computational fluid dynamic models). In both the UTTL and the NTTL, a spectral extinction coefficient β is assigned to each facet material type and transmission is computed using the Beer's equation,

$$\tau = e^{-\beta z} \tag{4}$$

where z represents the ray-traversed thickness for a given UTTL facet or the thickness traversed by a ray between two NTTL surface facets enclosing a volume. A spectral emissivity is also approximated by

$$\varepsilon = 1 - \tau \tag{5}$$

Although this constitutes a crude approximation, it allows for a spectral emissivity to be computed in cases where there are no direct measurements available. The next two sections will present two sample scenarios exercising the UTTL and NTTL cases in scenes rendered by DIRSIG.

4.0 CASE 1 - UTTL Forest Canopy

As stated in the previous section, the UTTL was designed to handle a class of transmissive targets that can be reduced to a two-dimensional primitive due in part to the predictable thickness of the facet. This is the assumption made for modeling leaf canopies. Figure 8 shows an example of a forest canopy rendering and a corresponding zoom of the scene.

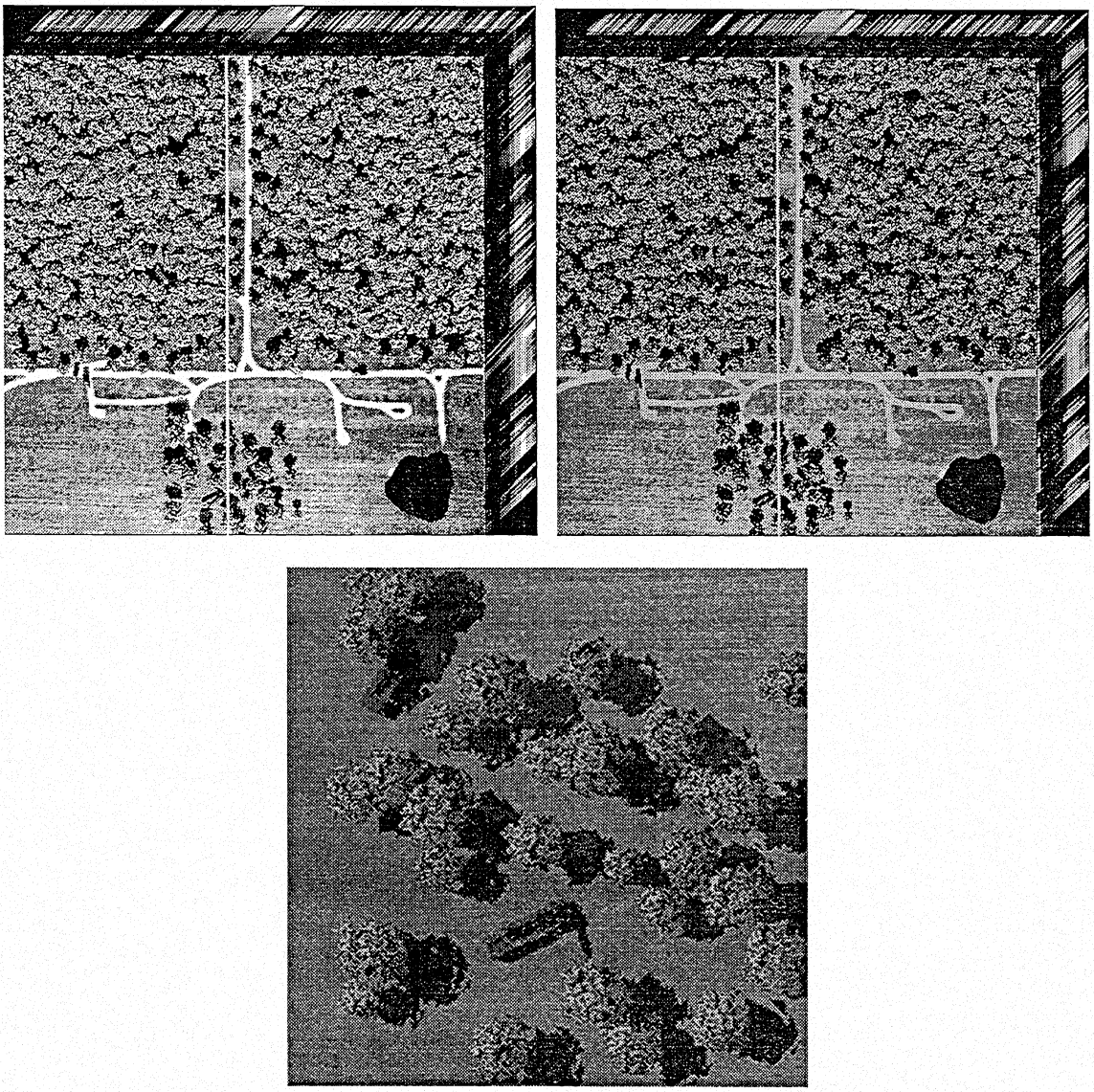

Figure 8 - Fifteen band M7 image cube of a simulated forest scene displayed as true color (top right), false color IR (top left), and a zoom of a region in the scene imaged at a different time of the day

This particular simulated forest scene contains several types of military vehicles in various stages of camouflage and obscuration. The two simulated images represent a 15 band multispectral simulation of the M7 sensor represented as data cubes with the true color and false color IR renditions for the front face of the data cube. The scene modeled contains approximately 600 tree crowns which have been approximated by 20-150 randomly distributed UTTL facets over a constrained dome volume representing each individual tree crown. For each facet, a spectral material emissivity and transmission was generated using the PROSPECT model[6] (based on Kubelka-Munk scattering theory) developed to predict the optical characteristics of leaves based on parameters such as leaf area index, moisture content, etc. Although no specific tree species was modeled, the crown geometry and leaf orientation can also be used as inputs into the DIRSIG model. The importance of the transmissive modeling combined with the complex radiometric interactions compounded by geometry (aside from the added realism) is revealed in the near infrared region between 0.8 and 2.0 microns where the effective reflectance increases dramatically. This is due in part to partial reflectance/transmittance

of the leaf layers in that region which produces a cascaded stacking effect that effectively increases the apparent reflectance of the canopy (*cf.* Figure 9).

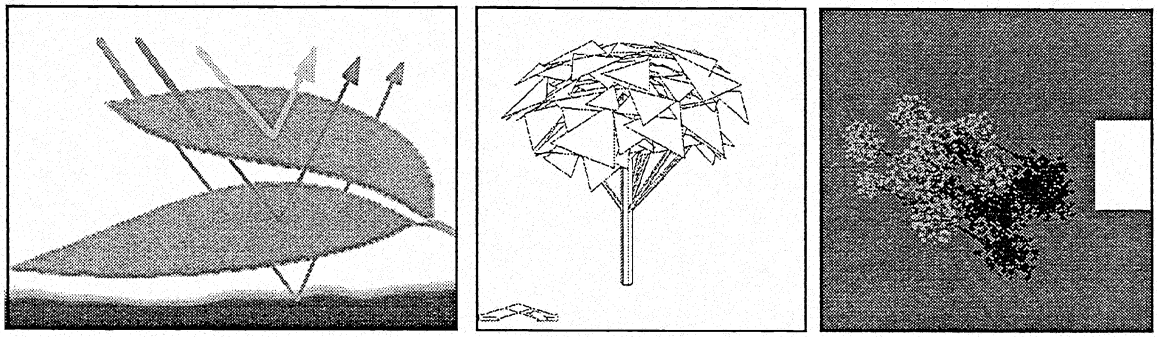

Figure 9 - Diagram showing the leaf stacking effects brought about by the partial transmission/reflectance of leaf layers, a sample wire frame of an individual tree canopy, and a sample rendering of a group of trees.

Likewise, self-shadowed regions are represented as dark magenta shades in the color IR as opposed to black shadows. The forest canopy example particularly exercises the integration of the UTTL data structure into DIRSIG because it generates numerous cases of ray-facet intersections for which contributing interactions need to computed. In general, the UTTL data structure is suited for applications containing well behaved and defined transmission regions such as littoral scenes characterized by stratified water layers. Current efforts are being conducted to test the applicability to such an example. In littoral scenes caused by more dynamic structure where both geometry and material properties follow less defined form, the NTTL data structure can be used as exemplified in the next section.

5.0 CASE 2 - NTTL Plume Model

There is a class of transmissive targets that generally involve fluid dynamics phenomena. These are characterized by amorphous regions segmented into volumes of approximately homogeneous fluid mechanic properties. The nature of the geometries can range from laminar to turbulent regions, many times involving several layers of volume region encapsulation. To address these types of targets, the NTTL data structure was designed. The specific scene example presented in this scenario is a primitive test case of an exhaust tower discharging steam. The tower and the surrounding structures and region are the same model used to generate Figure 1. In order for the steam plume to be appropriately modeled, a hydrodynamic plume code model obtained from the Los Alamos National Laboratories (adapted from the ANL/UI model[7]) was used to approximate the geometry of the plume along with the optical properties for a given set of input conditions, e.g., water droplet size distribution, surrounding air temperature, wind speed, etc. A sample wire frame of a plume generated by the LANL code is shown in Figure 10.

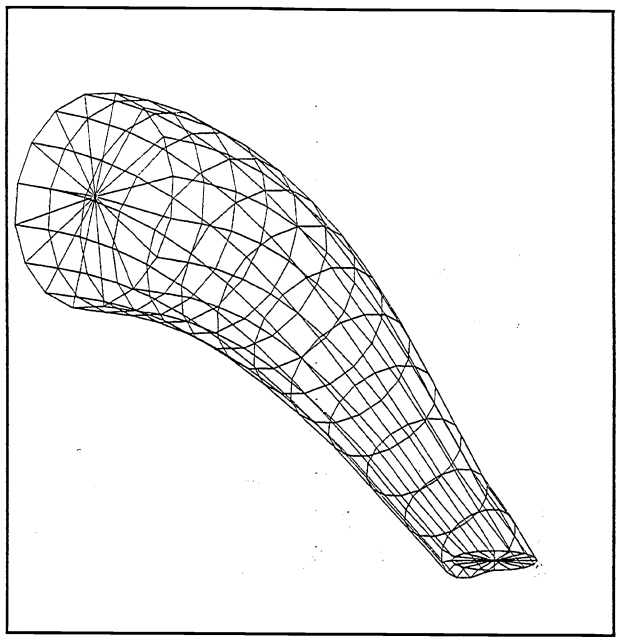

Figure 10 - Wire frame of plume geometry generated by LANL plume code

This wire frame was then attributed with the material and optical data generated by the LANL code and then inserted into the geometric database of the Hawkeye scene and then rendered by DIRSIG as a visible images (*cf.* Figure 11).

Figure 11 - DIRSIG renderings of LANL plume code generated model for different plume orientations

The renditions are 512 x 512 pixel true color simulated imagery based on the material/optical properties predicted by the LANL code. The two examples represent different geometric orientations of the plume having the same material/optical properties. These transmission plume images qualitatively illustrate that the trend of transmission effects follow a visually logical trend as indicated by the discernible, but hazily obscured houses

in the background and the varying shadow (caused by the plume's variation in thickness) cast onto the ground and lower objects. No texture variation has been applied to this imagery using the texture capabilities in DIRSIG and no shape factor computations to simulate earth shine has been applied. Although not tested by this specific scenario, the NTTL structure has the capability of modeling embedded laminar regions. Given the proper model to generate geometry and optical properties, application to meteorological clouds is conceptually straight forward.

6.0 Results and Recommendations

The implementation of transmissive scene elements has been incorporated successfully into DIRSIG and the resulting imagery reflects the expected behavior of transmissive objects manifested by transparency effects, shadow variations due to changing thickness, and cascaded stacking effects. The sample scenes presented simulating a forest canopy and the exhaust tower plume offer reasonable qualitative correlations to phenomena one might observe in corresponding real scenes. Both scenes prove the adequacy of the UTTL and the NTTL data structure in representing the geometry and material parameters of the facet elements to generate reasonably realistic synthetic scenes. A logical extension to other scenarios such as littoral scenes and meteorological clouds is also feasible provided that the appropriate materials and optical properties are available. Efforts are currently underway to prototype these scenes and obtain input data on the needed material properties. In addition, effort is being directed at enhancing the determination of optical properties such as spectral transmission and emissivity by implementing single and multiple scattering functions internal to the transmission volume based on scene specific orientations of the sun and scene elements.

As with all simulations and modeling, probably the weakest aspect falls on the quality of the material parameter inputs. Either the values are nonexistent or the quality of the data and the manner in which it was derived is suspect. To address this problem, a validation study involving imagery collection of a heavily instrumented scene will always be necessary to allow quantitative assessments to be performed on DIRSIG's ability to model truth.

In cases where the parameters are generated by a submodel, as in the PROSPECT model, additional validation outside of the DIRSIG model is required to insure that the generated data provides reasonably accurate information. For empirically determined data, a recommendation is made for data collection efforts to obtain calibrated imagery of the feature being measured (e.g. clouds, water, leaf layers, etc.) along with the necessary inputs into DIRSIG even if the main goal of the collection does not involve the use of the measured data in imaging. By obtaining the ancillary imagery and data, researchers can begin to use DIRSIG as a visualization, validation, and quality control tool for data collection efforts.

The spectral treatment of the radiometry in DIRSIG affords the ability to generate multispectral and even hyperspectral imagery of numerous scenes such as the ones presented. This potentially creates a source of well controlled input imagery into algorithms such as classification and spectral unmixing from which quantitative metrics of algorithm performance can be developed.

In summary, the implemented transmissive element methods provide reasonably credible imagery which qualitatively conform to expected phenomenology. Improvements to quantitative assessments will become possible as the quality of model input parameters become available and are subjected to more rigorous validation studies.

7.0 References

1. Schott, J.R., R.V. Raqueño, and C. Salvaggio, "Incorporation of a time-dependent thermodynamic model and a radiation propagation model into infrared three-dimensional synthetic image generation", Optical Engineering, Vol. 31, No. 7, 1992, pp. 1505-1516.

2. Salacain, J, S.D. Brown, R.V. Raqueño, and J.R. Schott, "Incorporation of sensor geometry effects in synthetic image generation model", *Ground Target Modeling and Validation Conference Proceedings*, Vol. I, pp. 420-434, August 1995.

3. Schott., J.R., S.D. Brown, R.V. Raqueño, T. Kraska, and R. White, "Validation and analysis of the Digital Imaging and Remote Sensing Laboratory's Synthetic Image Generation Model, DIRSIG", *Ground Target Modeling and Validation Conference Proceedings*, August 1996.

4. Mason, J.E., J.R Schott, and D. Rankin-Parobek, "Validation analysis of the thermal and radiometric integrity of RIT's synthetic image generation model, DIRSIG", *Proceedings of SPIE*, Vol. 2223, pp 474-487, Orlando, April 1994.

5. Schott, J.R., C. Salvaggio, S.D. Brown, and R.A. Rose, "Incorporation of texture in multispectral synthetic image generation tools", *SPIE Aerosense, Targets, and Backgrounds: Characterization and Representation*, Vol.. 2468, #23, Orlando, FL 1995.

6. Jacquemond, S. and F. Baret, "PROSPECT: A Model of Leaf Optical Properties Spectra.", Remote Sensing of Environment, Vol. 34, pp 75-91, 1990.

7. Carhart, R.A. and A.J. Policastro, "A Second-Generation Model for Cooling Tower Plume Rise and Dispersion - I. Single Sources", Atmospheric Environment, Vol. 25A, No 8, pp 1559-1576, 1991.